DE GRUYTER Biomedical Engineering
Biomedizinische Technik

Properties of different types of dry electrodes for wearable smart monitoring devices

Journal:	*Biomedical Engineering/Biomedizinische Technik*
Manuscript ID	BMT.2019.0167.R1
Manuscript Type:	Research Article
Date Submitted by the Author:	16-Oct-2019
Complete List of Authors:	Popović-Maneski, Lana; Institute of Technical Sciences of the Serbian Academy of Sciences and Arts, Ivanovic, Marija; VINCA Institute of Nuclear Sciences Atanasoski, Vladimir; University of Belgrade, Department of Biomedical Engineering and Technology Miletic, Marjan; VINCA Institute of Nuclear Sciences Zdolsek, Sanja; VINCA Institute of Nuclear Sciences Bojovic, Bosko; VINCA Institute of Nuclear Sciences Hadzijevski, Ljupco; VINCA Institute of Nuclear Sciences
Section/Category:	Basic Science Section
Classifications:	2.004 Biosignal Processing < 2 Biosignal Processing, Biomechanics, Image Processing, Modeling and Simulation, 5.002 Bioelectric and Biomagnetic Signals < 5 Diagnostic and Therapeutic Instrumentation, Clinical Engineering
Keywords:	dry electrodes, ECG, transient impedance, wearable monitor, motion artifacts, signal quality

Abstract:

Wearable smart monitors (WSM) applied for the estimation of electrophysiological signals are of utmost interest for a non-stressed life. WSM which records heart muscle activities could signalize timely a life-threatening event. The heart muscle activities are typically recorded across the heart at the surface of the body; hence, a WSM monitor requires high quality surface electrodes. The electrodes used in the clinical settings (i.e., Ag/AgCl with the gel) are not practical for the daily out of clinic usage. A practical WSM requires the application of a dry electrode with stable and reproducible electrical characteristics. We compared the characteristics of six types of dry electrodes and one gelled electrode during short term recordings sessions (☐30s) in real-life conditions: Orbital - monolithic polymer plated with Ag/AgCl, and five rectangular shapes 10×6×2mm electrodes (Orbital, silver electrode, silver/silver chloride electrode, gold electrode, and stainless-steel AISI304). The results of a well-controlled analysis which considered motion artifacts, line noise, and junction potentials suggest that among the dry electrodes Ag/AgCl performs the best. The Ag/AgCl electrode is in average three times better compared with the stainless-steel electrode often used in WSM.

Properties of different types of dry electrodes for wearable smart monitoring devices

Running head: Properties of dry electrodes

Lana Popović Maneski*, Marija D. Ivanović, Vladimir Atanasoski, Marjan Miletić, Sanja Zdolšek, Boško Bojović, Ljupčo Hadžievski

Lana Popović Maneski * (corresponding author: lanapm13@gmail.com)- Institute of Technical Sciences of the Serbian Academy of Sciences and Arts, Knez Mihailova 35/4, 11000 Belgrade, Serbia;

Marija D. Ivanović - Vinča Institute of Nuclear Sciences, Mike Petrovića Alasa 12-14, 11351 Belgrade, Serbia

Vladimir Atanasoski - Department of Biomedical Engineering and Technology, University of Belgrade, Studentski trg 1,11000 Belgrade, Serbia

Marjan Miletić - Vinča Institute of Nuclear Sciences, Mike Petrovića Alasa 12-14, 11351 Belgrade, Serbia

Sanja Zdolšek - Vinča Institute of Nuclear Sciences, Mike Petrovića Alasa 12-14, 11351 Belgrade, Serbia

Boško Bojović - Vinča Institute of Nuclear Sciences, Mike Petrovića Alasa 12-14, 11351 Belgrade, Serbia

Ljupčo Hadžievski - Vinča Institute of Nuclear Sciences, Mike Petrovića Alasa 12-14, 11351 Belgrade, Serbia

Abstract— Wearable smart monitors (WSM) applied for the estimation of electrophysiological signals are of utmost interest for a non-stressed life. WSM which records heart muscle activities could signalize timely a life-threatening event. The heart muscle activities are typically recorded across the heart at the surface of the body; hence, a WSM monitor requires high quality surface electrodes. The electrodes used in the clinical settings (i.e., Ag/AgCl with the gel) are not practical for the daily out of clinic usage. A practical WSM requires the application of a dry electrode with stable and reproducible electrical characteristics. We compared the characteristics of six types of dry electrodes and one gelled electrode during short term recordings sessions (≈30s) in real-life conditions: Orbital - monolithic polymer plated with Ag/AgCl, and five rectangular shapes 10×6×2mm electrodes (Orbital, silver electrode, silver/silver chloride electrode, gold electrode, and stainless-steel AISI304). The results of a well-controlled analysis which considered motion artifacts, line noise, and junction potentials suggest that among the dry electrodes Ag/AgCl performs the best. The Ag/AgCl electrode is in average three times better compared with the stainless-steel electrode often used in WSM.

Keywords—Dry electrodes; signal quality; ECG; wearable monitor; motion artifacts, transient impedance

Abbreviations

Ag/AgCl – silver/silver-chloride

ECG- electrocardiogram

EMG - electromyography

OM – output measure

PCB - printed circuit board

RMS – root mean square

WSM – wearable smart monitor

Introduction

Wearable smart monitors (WSM) are becoming practical tools for the improved quality of life because of the information and communication technologies development (miniaturization and online communication via smartphones or similar devices). The WSM of electrical potentials originating from the heart muscle could function as an on-line predictor of the need for an urgent intervention.

We show (Figure 1) examples of WSM used for the short-term recordings (up to 30s) of the electrocardiogram (ECG) that can be sent in the digital form to a remote center for inspection.

Figure 1. Examples of the hand-held ECG devices on the market: Kardia, AliveCor, US (left panel); CARDIO-B PALM ECG, GIMA, IT (middle panel), ECG check, Cardiac Designs, US (right panel). All three devices use stainless steel electrodes.

Many ECG WSM use stainless-steel electrodes touched by the fingers or palms of opposite arms (Lead I), but other types of dry electrodes made of different composites materials are emerging [1]. The commercially available ECG WSMs for short-term recordings measure the heart rate and, in some cases, detect the atrial fibrillations [2] from Lead I (records between the opposite hands). The new generation of ECG WSMs will allow automatic detection of much more, including the cardiac ischemia (ST segment shift) [3]. In this case, the ANSI standard for high-pass filtering must be followed (cutoff at 0.05 Hz), and raw signal quality is of utmost importance for obtaining high sensitivity and specificity of ischemia detection [4].

The WSM must measure the minimally distorted, noise-free electrophysiological signals, especially if the diagnostics are automatic without expert supervision. The critical points are the electrodes which transform the ionic to electron currents. The noise contaminating the recordings comes from power lines (50 or 60 Hz), motion artifacts due to movements or breathing, muscle electrical activities (EMG), short-term or long-term drifts due to temperature stabilization, the influence of light or changes in the electrode-skin impedances. To minimize the effects, a conductor covered with the hypo-allergic gel is being used. The gelled Ag/AgCl electrodes are considered as a golden standard. The chemical stability of the skin to

Ag/AgCl with gel interface minimizes most of the above-listed artifacts and allows the digital filtering to successfully “clean” the recordings [5,6]. However, the use of Ag/AgCl with gel is not practical, and most of the smart wearable devices tend to integrate reusable dry electrodes.

If dry electrodes are used, then the incidence of motion artifacts are much higher compared with the use of wet (pre-gelled) electrodes [4,7]. Also, dry electrode half-cell potentials on the electrode-skin junction and junction potentials between surface layers of the skin are time variable [8].

The current development of an ECG WSM required the analysis of the optimal dry electrodes. We focused on finding the optimal reusable dry electrodes that can be part of the printed circuit board (PCB) with minimal motion artifacts. In this paper, we present the performances of custom-made electrodes made of various types of metals that were mechanically compliant to our design such as stainless steel, silver, silver/silver chloride (Ag/AgCl) and gold. We did not consider rubber-based electrodes because they cannot be integrated into the PCB design. We compared the performances of the commercially available wet electrodes (Top Trace 51x33mm, Ceracarta, IT) and Orbital electrodes (Orbital Research Inc, Cleveland, OH, USA) [9]. The output measures were related to noise and motion artifacts in ECG-free signals recorded from the fingers since we investigated the electrical characteristics of the electrode-skin interface.

The characterization of electrodes in stationary conditions or long-term records is well documented in the literature [10,11], but the application of WSM held in hand does not belong to the stationary conditions. Therefore, we evaluated artifacts during the transitional changes of the electrode-skin interface (≈ 30 seconds from touching the electrodes). The frequency spectrum of ECG signals overlaps with artifacts; therefore, it is impossible to clearly separate ECG from the artifacts. If we record ECG-free signals with the same electrodes positioned at the same skin areas, then we measure only artifacts. These signals would simply superpose on the ECG action potentials when the ECG is measured. That is why we positioned the two electrodes at two fingers of the same hand to minimize the effects of electrophysiological signals (muscle activities and ECG). A similar method was suggested by Searle and Kirkup [10] who compared motion artifacts from three different pairs of electrodes by attaching them rigidly to the same housing with a fixed frequency vibrating element and placing them on the surface of one forearm. Our approach introduces three fundamental difference compared with what has been done: 1) the position of the electrodes was on the actual place where they are used for recording in ECG WSM (on the fingertips), 2) motion artifact was naturally induced in two typical positions of the forearm and 3) multiple output measures were calculated from the statistical analysis of the repeated recordings.

Methods

Protocol and instrumentation

Instrumentation. Custom designed holders for fingers (Figure 2, lower panel) supported seven sets of electrodes made of different materials and shapes (Figure 2, upper panel):

1. WET: a commercial wet electrode, Top Trace from Ceracarta (51x33 mm, metal contact diameter: 7 mm, hydrogel diameter: 17mm)
2. ORB: monolithic polymer plated with Ag/AgCl from Orbital (diameter: 25 mm, effective surface 500 mm^2 and pin height:150 µm, front to back resistance: 0.4 Ω)
3. ORB CUT: we cut Orbital electrode in the rectangular shape (10 x 6 x 2 mm) to fit our device design (front to back resistance: 8 Ω)
4. AG: a custom-made silver electrode in the same shape as ORB CUT (front to back resistance: 0.5 Ω)
5. AG/AGCL: a custom-made silver/silver chloride electrode in the same shape as ORB CUT (front to back resistance: 0.4 Ω)
6. AU: a custom-made gold electrode in the same shape as ORB CUT (front to back resistance: 0.5 Ω)
7. INOX: a custom-made stainless-steel (AISI304) electrode in the same shape as ORB CUT (front to back resistance: 0.5 Ω)

We chose the manufacture all metal electrodes in the shape of Orbital electrode because they can penetrate the hair on the chests in future use. The preparation of the custom-made electrodes was done in the institution workshop to avoid any edge effects. We present the results of the evaluation of the electrode-skin impedance for each type of electrode in Appendix.

Figure 2. Upper panel: electrode types, lower panel: measurement setup. Recordings were made between the thumb and middle finger of one hand (no ECG, only noise, and artifacts) in two positions: arm supported on the table and elbow supported with the forearm in the upright position.

A host computer operating in the Windows environment captured signals. The digital amplifier which integrates a 24-bit A/D converter (ADS1298, Texas Instruments, TX, USA) with the gain of the input instrumentation amplifiers set at A = 12, in the DC coupled mode was connected to the electrodes.

Subjects: Ten volunteers (4 men and 6 women, age 35±11, BMI 23.9 ± 4.3) with no known skin, adipose tissue, vascular disorder or pathological tremor volunteered in the study. All subjects signed the informed consent approved by the Ethics Committee of the Medical School, University of Belgrade, Belgrade.

Protocol: The subjects were sitting comfortably next to a table, with one elbow supported by the table. The measurements included two setups (Figure 2, lower panel): 1) the forearm was resting on the table, and the subject was holding the electrodes on the sides of the device with his/her thumb and middle finger, and 2) the forearm was pointing against the gravity. Subjects were instructed to relax as much as possible (a minimum contraction of forearm muscles and no motion). Three sessions, lasting 30s each, were recorded for both setups. In total, 420 sets of signals were recorded (6 per subject × 7 electrode types × 10 subjects), or 6×10×30=1800s of recordings in natural conditions per each electrode type.

Data analysis

All data processing was done in Matlab 2014b (Mathworks, Natick, USA). We used six recordings per electrode type per subject to estimate the mean±std (standard deviation) values for each output measure. All records were heuristically inspected for unlikely irregularities (e.g. excess 50 Hz noise due to poor contact, recording interrupted or subject moved during recording). If the inspection suggested high contamination by the noise of non-physiological source other than 50 Hz, then these signals were excluded from the further analysis.

As there was a substantial difference in absolute values between subjects, we normalized values for all electrodes in each subject with the following formula:

$$OM_i^{NORM} = \frac{OM_i}{\sum_{j=1}^{7} OM_j}$$

where OM is output measure, and *i* and *j* are representing the type of electrode.

Seven different output measures were developed to quantify various aspects of noise and artifacts in ECG recordings and their influence on proper ECG signal reading and diagnosis. Signal processing steps and output measures (OM) were the following:

1. OM 1: The RMS value of 50 Hz power-line noise (a band-pass filtered original signal with 3rd order Butterworth filter between 48-52 Hz)

2. OM 2: The RMS value of 6-13 Hz tremor (a band-pass filtered original signal with 3rd order Butterworth filter between 6-13 Hz). Physiological tremor is expected oscillatory motion in fingers of all healthy individuals in the frequency range of 6-13Hz with different amplitudes depending on the current physiological and psychological conditions [12,13].

3. The component of the signal from the muscle activities (EMG): After subtracting 50 Hz noise and tremor (same filtered signals which were used to calculate OM 1 and OM 2) from the original signals, the signals were low-pass filtered with 3rd order Butterworth filter at 30 Hz to remove EMG signals. EMG frequency range is 30-300 Hz. EMG component can be seen in Fig.3A.

4. The high-pass filtered (HPF) signals at: a) 0.05 Hz (FIR filter with order 4496) or b) 1 Hz (3rd order Butterworth filter). We selected the cutoff frequency at 0.05 Hz based on standards for devices used for detection of ischemia (ST shift) and other heart pathologies. The 1 Hz cutoff was chosen for detection of heart rhythm (occurrence of QRS segments).

5. OM 3: The RMS values of the signals after the high-pass filtering. These values provide a measure of total baseline wandering during 30s recording (there was no ECG in the recorded signals). Large

baseline wandering can make ECG signal reading difficult if there is no auto-scaling function on the reading device.

6. OM 4: The histograms with 7 BINs after each type of high-pass filtering:

(1) BIN001: number of samples with values ≤0.01mV

(2) BIN005: number of samples with values between 0.01mV-0.05mV

(3) BIN01: number of samples with values between 0.05mV-0.1mV

(4) BIN02: number of samples with values between 0.1mV-0.2mV

(5) BIN05: number of samples with values between 0.2mV-0.5mV

(6) BIN1: number of samples with values between 0.5mV-1mV

(7) BINout: number of samples with values >1mV (typical amplitude of QRS segment recorded on the surface of the skin)

7. The duration of intervals in which all consecutive samples are smaller than 0.1mV after each type of high-pass filtering. This threshold was selected because it represents a minimal ST shift that can be interpreted as pathological [14]. This segment was named a "good" signal interval. OM 5: We calculated the longest "good" interval.

8. OM 6: The number of "good" segments lasting at least 5s for after each type of high-pass filtering. The duration of 5s was selected because in the most common case there would be at least five heartbeats within 5s. If the signal is artifact free during this period, it should be enough for a cardiologist to notice if there are any essential changes in the shape (not rate) of the ECG signal.

9. OM 7: The number of “good” segments lasting at least 2s after each type of high-pass filtering. The duration of 2s was selected because in general case there would be at least one heartbeat within 2s. Considering that the ECG signal can be randomly contaminated with noise and artifacts, if there were multiple 2s “good” intervals, then they can be selected to form a sequence of good quality heartbeat signals for the proper diagnosis of potential ischemia by the cardiologist.

Examples of how we calculated the number of "good" segments are the following: if a good segment (all values <0.1mV) lasts 3s than it contains one 2s "good" segment and none of 5s "good" segments. If a "good" segment lasts 6s, then it includes three 2s "good" segments and one 5s "good" segment. If there are two "good" segments lasting 2s and 6s, then the recording contains four 2s "good" segments and one 5s "good" segment.

Statistical analysis was done in an Excel Xlstat program (Microsoft Office). Data were tested for normality with the Shapiro-Wilk normality test. Due to the relatively small sample size in the experiments, we used non-parametric tests. The Kruskal-Wallis test tested the significance of the results for independent samples with the significance level p=0.05.

Results and discussion

The graphical presentation of all calculated output measures is shown in Figure 3. The heuristic examination of signals resulted in the exclusion due to biological noise of just over 5% of the recorded signals (22 out of 420 recordings).

Different RMS values for all subjects and all electrodes are shown in Figure 4.

Figure 3. All output measures of the recorded signals. A) Original signal and components originating from 50 Hz power line noise, 6-13 Hz tremor and EMG (>30 Hz), B) Power spectrum of original signal and the same signal after removing 50 Hz noise, tremor and EMG components, C) Longest "good" interval (low and high red marks showing beginning and end of the "good" interval) and other "good" intervals (green marks) for signal high-pass filtered at 0.05 Hz, D) Seven-BIN histogram after high-pass filtering at 0.05 Hz, E) Longest "good" interval (red marks showing beginning and end or interval) and other "good" intervals (green marks, none in this case) for signal high-pass filtered at 1 Hz, F) Seven-BIN histogram after high-pass filtering at 1 Hz

Figure 4. Absolute RMS values of different signal components originating from: power line noise between 48-52 Hz, motion artifact due to physiological tremor between 6-13 Hz, baseline wandering after removing 50 Hz noise and tremor and band-pass filtering between 0.05-30 Hz or 1-30 Hz. Standard deviations show the variability of results from 6 recordings in each subject. Numbers next to individual bars represent values of the bar that is out of the presented range.

Summary statistics for each electrode type and each output measure are shown in Figure 5. The normalized values for all electrodes in each subject (e.g., in Figure 4, RMS of 50 Hz noise for subject 4, on AU and WET electrodes, is 0.47±0.25mV and 0.03±0.01mV, which equals to 33.9±18.3% and 1.9±0.9%

when normalized for subject 4, respectively) were used to calculate mean±std values for all subjects for each electrode type (Figure 5).

Figure 5. Summary statistics for different output measures for seven electrode types. Top panels show a comparison of normalized RMS values of 50 Hz noise and tremor motion artifact. After low-pass filtering at 30 Hz and high-pass filtering at 0.05 Hz (gray side) or 1 Hz (red side) RMS values quantify baseline wandering. Stacked bar plots represent values from the histograms divided into seven custom BINs. The length of the "good" segment (all samples in segment <0.1mV) is shown relative to the length of the whole recording (the 30s). The number of “good” segments lasting at least 5s or 2s are shown in bottom panels as orange and blue bars, respectively.

The orbital electrode in original form (ORB) and AG picked up the least of 50 Hz noise compared to other dry electrodes. Cutting Orbital (ORB) to rectangular shape resulted in 45% more noise, which was expected as decreasing the contact surface *per se* increases the impedance, which lowers the signal-to-noise ratio. Also, by cutting the surface conductive layer, we may have deteriorated the characteristics of the applied technology. AG/AGCL electrode picked up 5% less noise than ORB CUT. There was no statistically significant difference between AG/AGCL, ORB, ORB CUT, and AG electrodes. AU and INOX performed significantly worse than other tested electrodes.

WET, AG/AGCL and ORB induce similar RMS values of tremorous finger motion between 6-13 Hz, while ORB CUT and AG recorded slightly larger amplitudes. AU and INOX performed significantly worse.

After high-pass filtering at 0.05 Hz the RMS value of the baseline wandering was the minimal for ORB (7.04%), followed by AG/AGCL (8.29%), ORB CUT (8.54%), AG (10.77%), AU (20.59%) and INOX (41.13%) compared to WET (3.64%). After high-pass filtering at 1 Hz the RMS value of the baseline wandering was minimal for AG/AGCL (7.45%), followed by ORB (8.31%), ORB CUT (10.54%), AG (10.84%), AU (20.59%) and INOX (37.01%) compared to WET (5.25%). AU and INOX were statistically worse than other electrodes in both cases of filtering.

After high-pass filtering at 0.05 Hz (clinical standard) ORB, ORB CUT, and AG/AGCL had a similar number of samples in all BINS. ORB had the highest number of samples in first three BINs (values up to 0.1mV) (70.88%) compared to WET (82.97%). AG/AGCL (67.93%) and ORB CUT (65.93%) followed.

After high-pass filtering at 1 Hz (dynamic filtering), AG/AGCL had the highest number of samples in first BIN (values up to 0.01mV) following the WET closely. However, the number of samples in first BIN is irrelevant in the applications in which 1 Hz filtering is justified.

Histograms and quantity of low-value BINs are essential for distinguishing if the electrodes are more or less prone to noise and baseline wandering. Histograms are not good indicators of unpredicted abrupt changes in signals. For this purpose, we developed a new measure - the duration of "good" parts of a signal (where all the consecutive values are smaller than 0.1mV). After high-pass filtering at 0.05 Hz, the longest "good" interval in the 30s recording was obtained with AG/AGCL (9.08±5.67s) compared with WET (15.78±10.07s). AG (7.96±6.82s) and ORB CUT (7.95±3.39s) had better behavior than ORB (6.99±4.63s). AU and INOX barely had any 2s "good" intervals. After high-pass filtering at 1 Hz, the average duration of the longest "good" part of the signal was the best for AG/AGCL (24.6±4.06s) compared with WET (26.74±5.78s). AG had the highest number of "good" segments lasting at least 5s each (4.75±2.41s), but the results for WET, AG/AGCL, ORB, ORB CUT and AG were comparable. AU and INOX performed worse.

Results of the signal quality analyses are not all in line with the results of electrode-skin impedances presented in the Appendix. An example is that AG/AGCL electrode had high values of impedance, but still recorded well the signals from the skin surface. This statement is in line with Chi et all. [1] presenting that the low resistance (high conductance) is not essential for the good electrode performance, and that maximizing resistance (minimizing conductance) in electrode-skin coupling could be beneficial in specific cases.

The results in favor of Ag/AgCl based electrodes are following our previous work (unpublished results). We tested ORB CUT electrode performance in a study that included 2096 recordings from 34 subjects using prototype hand-held devices in the home environment. We found that the signal quality was acceptable for detection of ST shift in 95% of the recordings.

Conclusion

We compared the performance of different dry, eventually PCB mountable, non-expensive materials that could be used as dry electrodes in ECG WSM. The golden standard is Ag/AgCl electrode with gel, described in the literature *[15]*. We measured the signals coming from the body at the skin with different dry electrodes in real-life situations and classified them into seven metrics. The results suggest that Ag/AgCl based electrodes perform best regardless of the shape and large inter-subject variability. ORB minimizes the power line noise, introduces small base-line wandering and allows the most extended good quality recording sections when compared to other dry electrodes. The next in line are Ag/AgCl dry electrodes picking up little more power line noise and comprising a most substantial number of short sequences of good quality signals. Electrodes based on other materials showed worse characteristics in our measurements. INOX performed the worse in all metrics.

Filtering at 1 Hz substantially lowers the baseline wandering and other motion artifacts, leading to less differentiation in the behavior of different dry electrodes compared to each other and compared to wet electrodes. That means that in applications such as detection of heart rate or atrial fibrillations with high-pass filtering at 1 Hz the use of INOX electrodes may be justified as an acceptable tradeoff between the price, durability, and quality. However, for the applications in ECG WSM with algorithms for automatic detection of cardiac ischemia and other heart diseases based on the assessment of the morphology of the ECG signals, the ANSI standard for high-pass filtering must be followed (high-pass filtering limit at 0.05 Hz). In those applications, much better performance can be achieved with Ag/AgCl based electrodes.

We used 7 metrics to evaluate the characteristic of dry electrodes made of different materials. Depending on the application, different metrics can be more important. For instance, if the electrode is used in WSM device to automatically detect ischemia (with HPF at 0.05 Hz) then the most significant differences are found in the number of 5s segments with all signals <0.1mV. If the WSM is used to detect arrythmias (with HPF at 1 Hz) than the most significant differences are found in RMS values after filtering. The results of our study suggest that the electrode-skin impedance is not necessarily a good indicator of the electrode performance for short term recordings.

Appendix

Electrode-skin impedance was measured in the 10 subjects described earlier, with the experiment setup shown in Figure 6. OP177 is an operational amplifier (OP) with the high input impedance (45 MΩ). One electrode was connected to the negative input of OP and other electrode of the same type was connected to the output of the OP. Electrode pairs were positioned on a plexiglass plane. Subject touched with his/her left and right index finger two electrodes of the same type on different planes.

V_{in} is a complex low-voltage periodic signal composed of 22 sine waves at different frequencies, described by the term:

$$V_{in} = \sum_{i=1}^{22} 0.5 * \sin(2\pi i^2)$$

V_{in} was generated as an analogue output on NI6363 USB DAQ board, in LabView program (National Instruments, Texas). For each subject $R_{current}$ was selected to one of the values [500KΩ, 5MΩ, 50MΩ] based on the highest values of impedance in the subjects to avoid saturation of V_{out} and optimize the resolution of 16 bit AD conversion. V_{out} was acquired on one analogue input by the same LabView program. Each acquisition lasted 40s. Subject placed the fingers on electrodes after the acquisition started, to ensure the recordings from the instant when the skin touched the electrode (example in Figure 7A). After touching the electrodes the palms were resting on the plexiglass board to minimize the motion.

Figure.6. Experiment setup for recording of electrode-skin impedance and model of the electrode-skin interface (modified from [1]). E_{hc} is a half-cell potential due to interaction of the skin humidity and sweat with the electrode.

From the recorded signals the program automatically detected the instant when the skin touched the electrodes, as the position of time window of width f_s (f_s is sampling rate) in which the equation:

$$\max(V_{out}) < 0.5 * max(V_{in})$$

was satisfied for the first time (black line in Figure 7A).

We calculated Fourier Transform (FFT) of V_{in} and V_{out} in time windows of $2*f_s$ (example in Figure 7B):

$$F_{in}[j] = FFT\{V_{in}[k]\}$$

$$F_{out}[j] = FFT\{V_{out}[k]\}$$

Impedance was calculated from the formula:

$$Z = \frac{F_{out}}{R_{current} * F_{in}}$$

The impedance values for time windows [0, 2s], [3s, 5s], [15s, 17s] and [28s, 30s] are shown in Figure 7C (real and imaginary parts) and 7D (absolute values). Transitional time behaviors of impedances for selected frequencies ($|Z(j)|$, where j corresponds to frequencies of 1, 3, 8, 16, 25 and 81 Hz) are shown in Figure 7E. The same trends were found in all subjects. The only differences were the maximum and minimum values of the impedance (Figure 8).

Figure 7. Results of electrode-skin impedances for different electrodes in one subject. Presented values are for two electrode-skin contacts in series (two fingers on two different electrodes).

Figure 8. Minimum and maximum electrode-skin impedance absolute values from all subjects. All the values are doubled.

Author statement

Research funding: The work on this project was partly supported by the grants III44008 and III45010 from the Ministry of Education, Science and Technological Development of Serbia, Belgrade.

Conflict of interest: Authors state no conflict of interest.

References

[1] Chi YM, Jung T-P, Cauwenberghs G. Dry-Contact and Noncontact Biopotential Electrodes: Methodological Review. IEEE Rev Biomed Eng. 2010;3:106–19.

[2] Mehta DD, Nazir NT, Trohman RG, Volgman AS. Single-lead portable ECG devices: Perceptions and clinical accuracy compared to conventional cardiac monitoring. J Electrocardiol. 2015 Jul;48(4):710–6.

[3] Guo S-L, Han L-N, Liu H-W, Si Q-J, Kong D-F, Guo F-S. The future of remote ECG monitoring systems. J Geriatr Cardiol JGC. 2016;13(6):528–30.

[4] Kligfield P, Gettes LS, Bailey JJ, Childers R, Deal BJ, Hancock EW, et al. Recommendations for the standardization and interpretation of the electrocardiogram: part I: the electrocardiogram and its technology a scientific statement from the American Heart Association Electrocardiography and Arrhythmias Committee, Council on Clinical Cardiology; the American College of Cardiology Foundation; and the Heart Rhythm Society endorsed by the International Society for Computerized Electrocardiology. J Am Coll Cardiol. 2007;49(10):1109–27.

[5] Enderle JD, Bronzino JD, editors. Introduction to biomedical engineering. 3rd ed. Amsterdam ; Boiston: Elsevier/Academic Press; 2012. 1252 p.

[6] Webster JG, Clark JW, editors. Medical instrumentation: application and design. 4th ed. Hoboken, NJ: John Wiley & Sons; 2010. 713 p.

[7] Meziane N, Webster JG, Attari M, Nimunkar AJ. Dry electrodes for electrocardiography. Physiol Meas. 2013;34(9):R47-69.

[8] Macy A. The Handbook of Human Physiological Recording, Chapter 4: Electrodes. Referenced. 2015;7:2017 [Internet]. Available from: https://alanmacy.com/books/the-handbook-of-human-physiological-recording/chapter-4-electrodes/

[9] Albulbul A. Evaluating Major Electrode Types for Idle Biological Signal Measurements for Modern Medical Technology. Bioeng Basel Switz. 2016 Aug 24;3(3).

[10] Searle A, Kirkup L. A direct comparison of wet, dry and insulating bioelectric recording electrodes. Physiol Meas. 2000;21(2):271–83.

[11] Baek J-Y, An J-H, Choi J-M, Park K-S, Lee S-H. Flexible polymeric dry electrodes for the long-term monitoring of ECG. Sens Actuators Phys. 2008;143(2):423–9.

[12] Raethjen J, Pawlas F, Lindemann M, Wenzelburger R, Deuschl G. Determinants of physiologic tremor in a large normal population. Clin Neurophysiol Off J Int Fed Clin Neurophysiol. 2000;111(10):1825–37.

[13] Mario M, Giuliana G, Thomas L, Dario F, Lana P, Silvia C, et al. Bioinformatic Approaches Used in Modelling Human Tremor. Curr Bioinforma. 2009;4(2):154–72.

[14] Malik M, Camm AJ, editors. Dynamic electrocardiography. 1st ed. Elmsford, N.Y: Blackwell; 2004. 637 p.

[15]Geddes LA, Baker LE. Principles of applied biomedical instrumentation. 3rd ed. New York: Wiley; 1989. 961 p.

Fig. 1. Examples of the hand-held ECG devices on the market: Kardia, AliveCor, US (left panel); CARDIO-B PALM ECG, GIMA, IT (middle panel), ECG check, Cardiac Designs, US (right panel). All three devices use stainless steel electrodes.

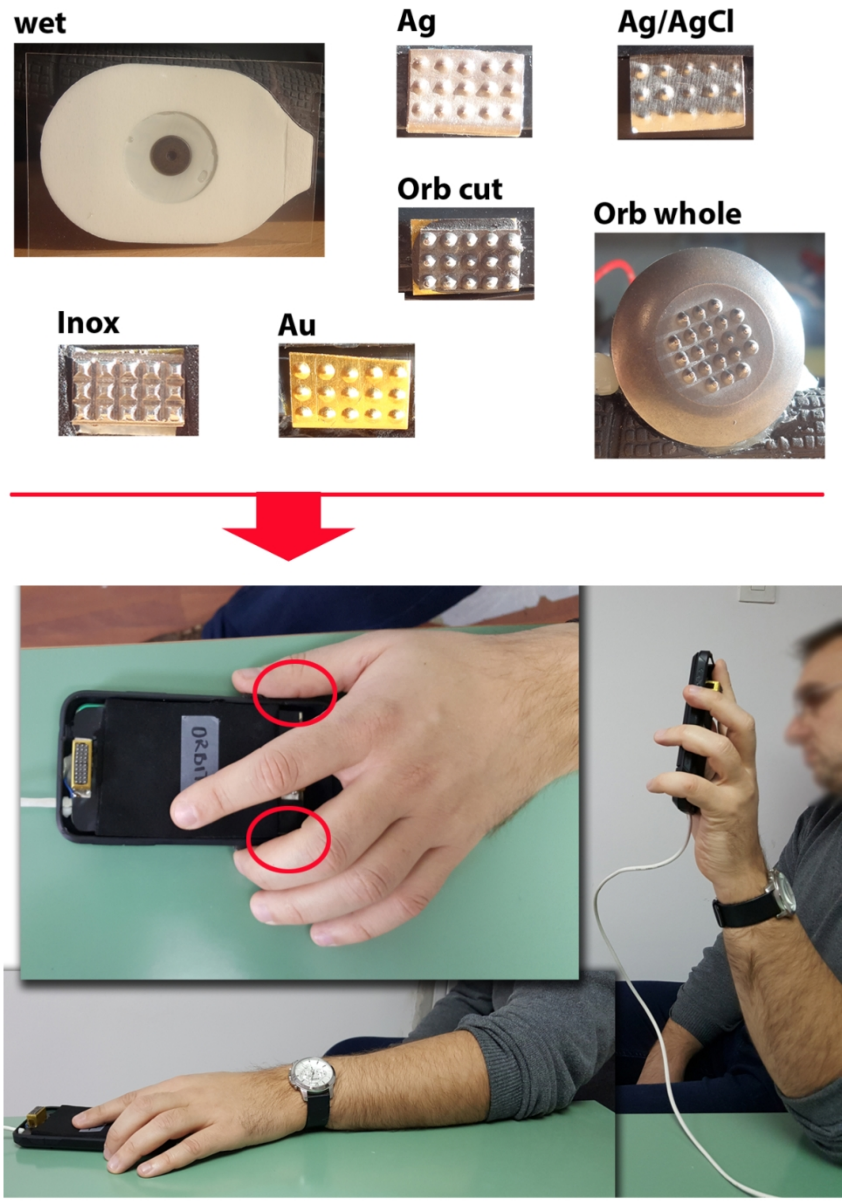

Fig. 2. Upper panel: electrode types, lower panel: measurement setup. Recordings were made between the thumb and middle finger of one hand (no ECG, only noise, and artifacts) in two positions: arm supported on the table and elbow supported with the forearm in the upright position.

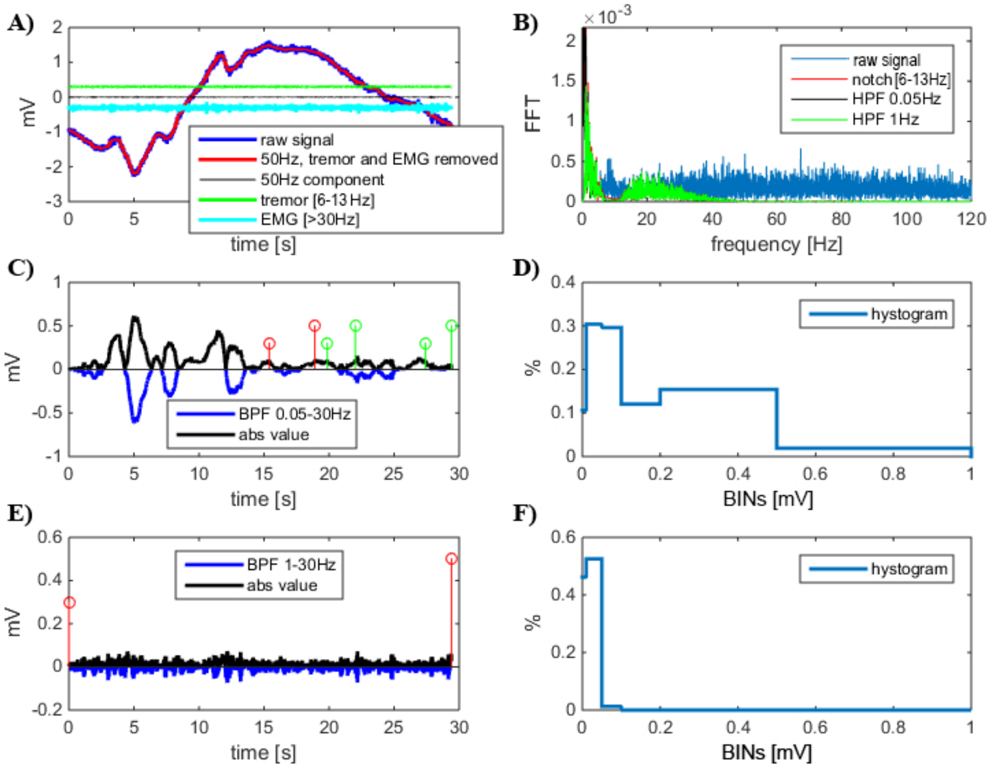

Fig. 3. All output measures of the recorded signals. A) Original signal and components originating from 50Hz power line noise, 6-13Hz tremor and EMG (>30Hz), B) Power spectrum of original signal and the same signal after removing 50Hz noise, tremor and EMG components, C) Longest "good" interval (low and high red marks showing beginning and end of the "good" interval) and other "good" intervals (green marks) for signal high-pass filtered at 0.05Hz, D) Seven-BIN histogram after high-pass filtering at 0.05Hz, E) Longest "good" interval (red marks showing beginning and end or interval) and other "good" intervals (green marks, none in this case) for signal high-pass filtered at 1Hz, F) Seven-BIN histogram after high-pass filtering at 1Hz

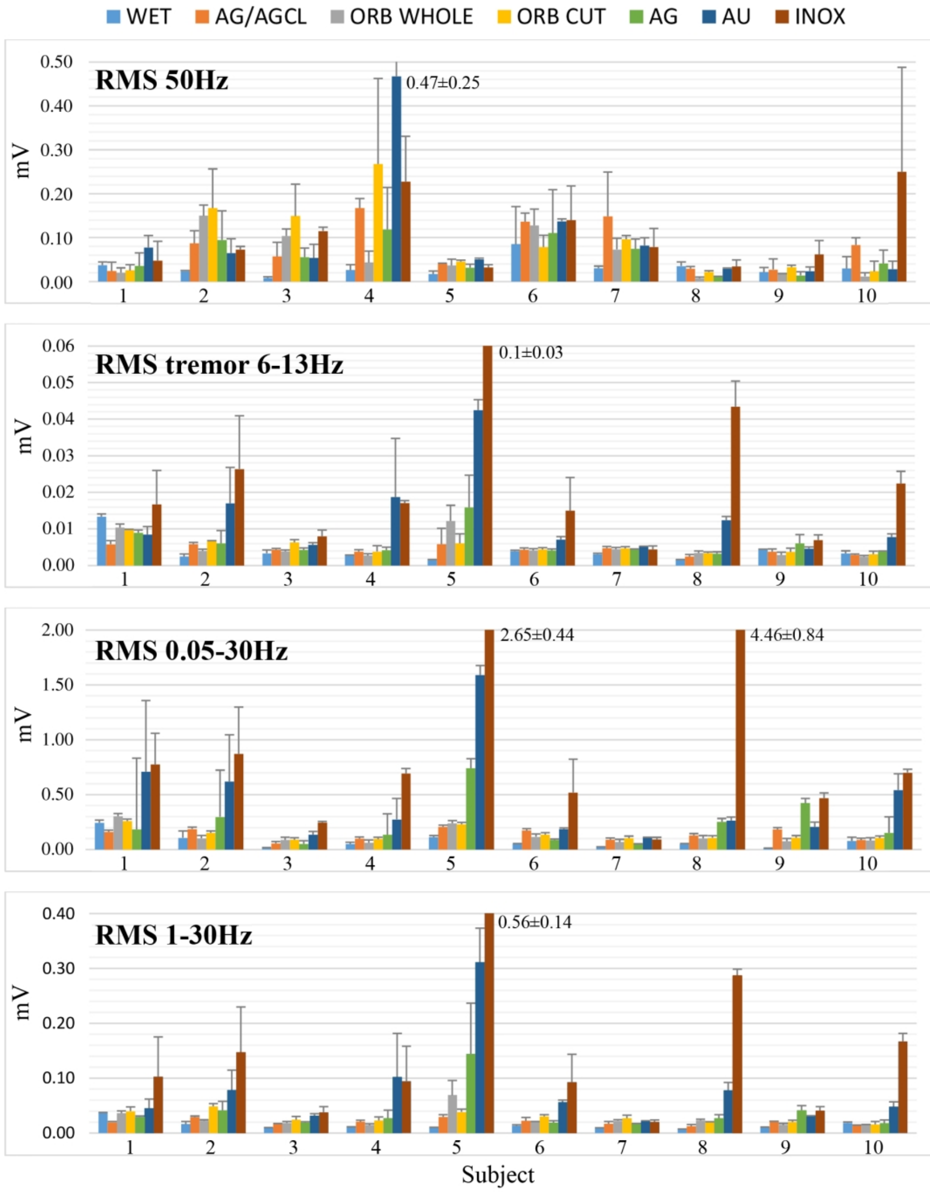

Fig. 4. Absolute RMS values of different signal components originating from: power line noise between 48-52Hz, motion artifact due to physiological tremor between 6-13Hz, baseline wandering after removing 50Hz noise and tremor and band-pass filtering between 0.05-30Hz or 1-30Hz. Standard deviations show the variability of results from 6 recordings in each subject. Numbers next to individual bars represent values of the bar that is out of the presented range.

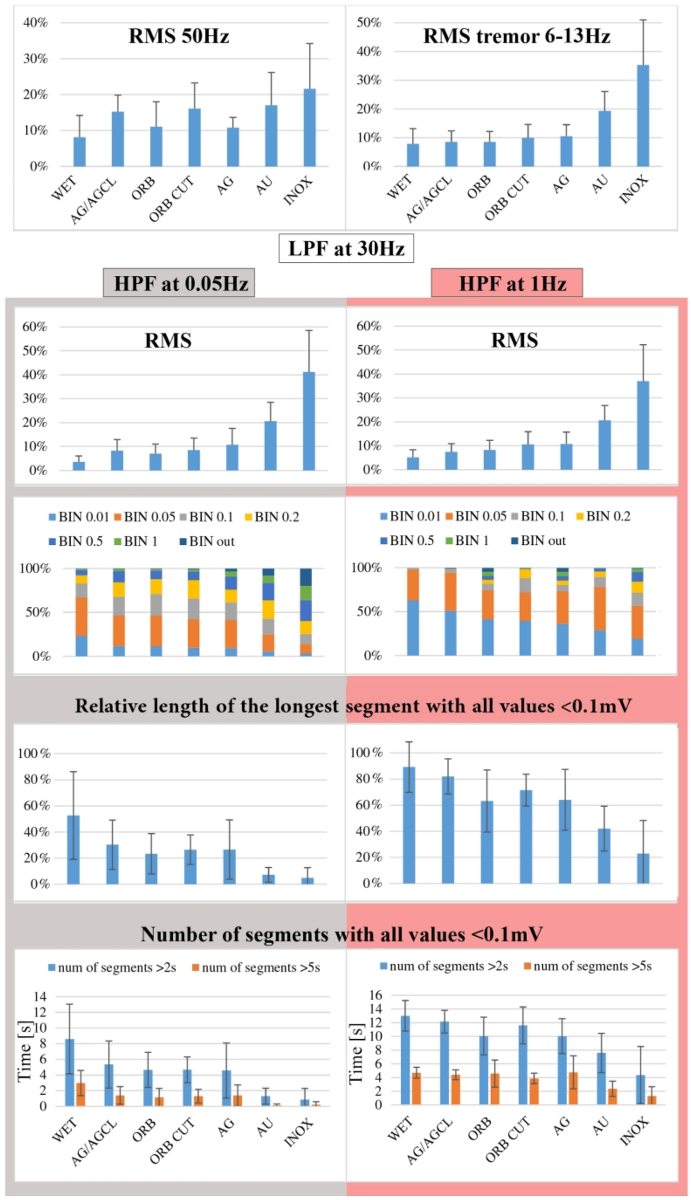

Fig. 5. Summary statistics for different output measures for seven electrode types. Top panels show a comparison of normalized RMS values of 50Hz noise and tremor motion artifact. After low-pass filtering at 30Hz and high-pass filtering at 0.05Hz (gray side) or 1Hz (red side) RMS values quantify baseline wandering. Stacked bar plots represent values from the histograms divided into seven custom BINs. The length of the "good" segment (all samples in segment <0.1mV) is shown relative to the length of the whole recording (the 30s). The number of "good" segments lasting at least 5s or 2s are shown in bottom panels as orange and blue bars, respectively.

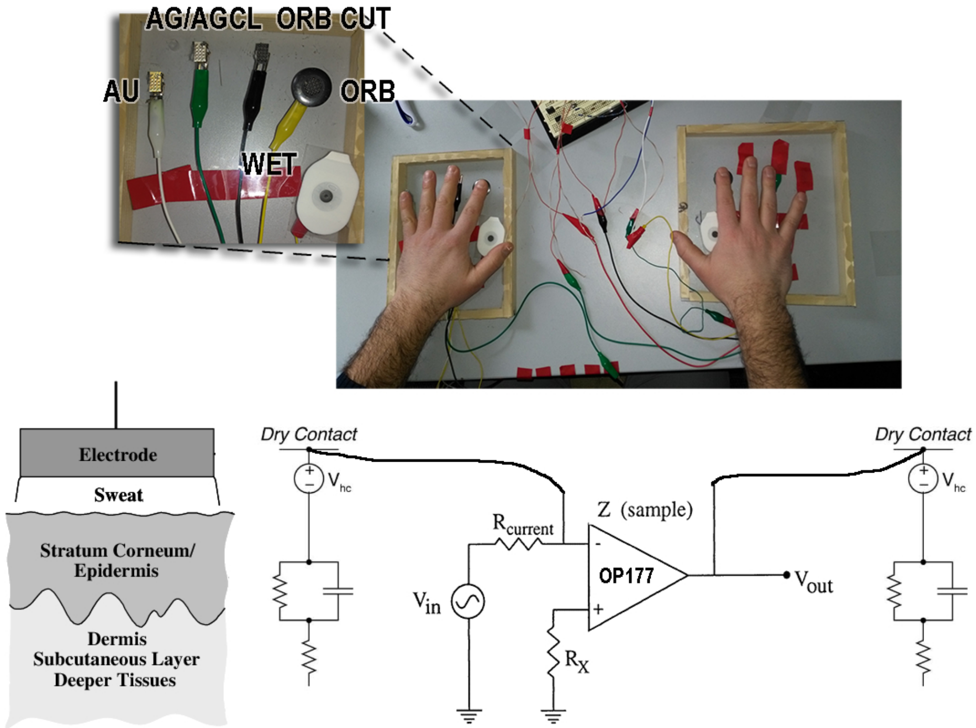

Figure 6. Experiment setup for recording of electrode-skin impedance and model of the electrode-skin interface (modified from [16]). Ehc is a half-cell potential due to interaction of the skin humidity and sweat with the electrode.

386x295mm (72 x 72 DPI)

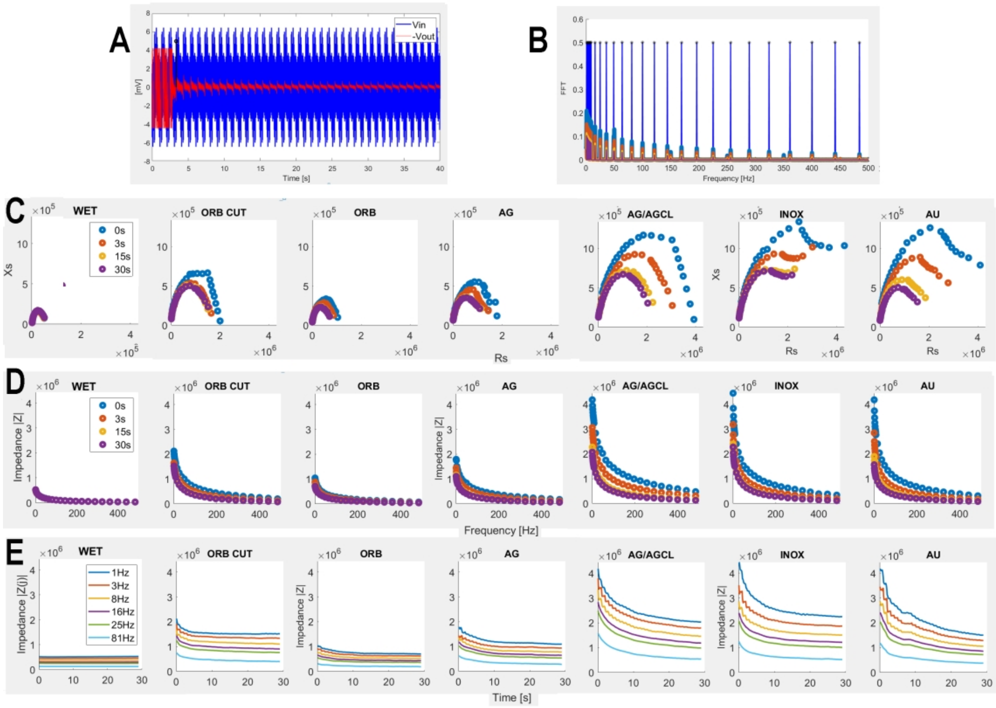

Figure 7. Results of electrode-skin impedances for different electrodes in one subject. Presented values are for two electrode-skin contacts in series (two fingers on two different electrodes).

237x170mm (300 x 300 DPI)

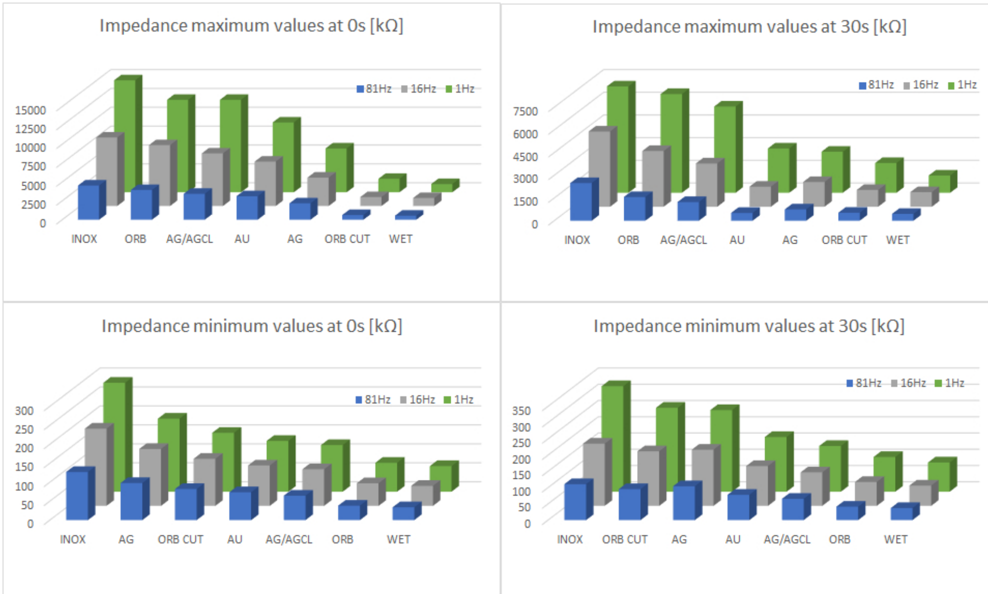

Figure 8. Minimum and maximum electrode-skin impedance absolute values from all subjects. All the values are doubled.

122x73mm (200 x 200 DPI)